Geophysical Research Letters

RESEARCH LETTER
10.1029/2024GL111442

Tracking 3D Drought Events Across Global River Basins: Climatology, Spatial Footprint, and Temporal Changes

Xin Feng[1], Zhaoli Wang[1,2], Xushu Wu[1], Shengzhi Huang[3], Jun Li[4], Chengguang Lai[1,2], Zhaoyang Zeng[1], and Guosheng Lin[5]

[1]School of Civil Engineering and Transportation, State Key Laboratory of Subtropical Building Science, South China University of Technology, Guangzhou, China, [2]Pazhou Lab, Guangzhou, China, [3]State Key Laboratory of Eco-Hydraulics in Northwest Arid Region of China, Xi'an University of Technology, Xi'an, China, [4]Sino-French Institute for Earth System Science, College of Urban and Environmental Sciences, Peking University, Beijing, China, [5]Agricultural Machinery Station, Meizhou, China

Key Points:

- Drought changes between 1979–1999 and 2000–2020 are insignificant in most basins
- Amazon, Nile and La Plata basins experienced higher drought severity than other basins
- Drought affected area and severity generally increased with duration for most basins

Supporting Information:

Supporting Information may be found in the online version of this article.

Correspondence to:

X. Wu,
xshwu@scut.edu.cn

Citation:

Feng, X., Wang, Z., Wu, X., Huang, S., Li, J., Lai, C., et al. (2025). Tracking 3D drought events across global river basins: Climatology, spatial footprint, and temporal changes. *Geophysical Research Letters*, *52*, e2024GL111442. https://doi.org/10.1029/2024GL111442

Received 19 JUL 2024
Accepted 30 JAN 2025

Abstract Understanding the spatial and temporal patterns of drought is essential for mitigating drought-induced impacts. To date, less attention is paid to drought characterization and changes across global river basins within a 3D clustering drought identification framework. Here, we characterized drought events across 59 global river basins during 1979–2020 based on standardized precipitation evapotranspiration index and a three-dimensional clustering method, together with exploration of relationships between drought indicators. The results show that drought characteristics did not change significantly over time in most basins, but the frequency tended to decrease in the Middle East and North Africa and showed increase at high latitudes. Droughts in Amazon, Nile and La Plata basins are severer than other basins with higher severities on the whole. Moreover, for most all basins, drought affected area and severity both increased with duration.

Plain Language Summary Understanding space and time characteristics of drought is crucial for reducing the impacts of drought. Until now, we have paid less attention to drought characterization and change in river basins around the world from the three-dimensional perspective. Here, we used the Standardized Precipitation Evapotranspiration Index tool and a three-dimensional clustering method, to identify drought events between 1979 and 2020 in 59 global river basins, and explored the relationships between drought intensity, severity, duration and affected area. Our findings showed that most basins did not experience significant changes in drought characteristics over time. However, the frequency of droughts decreased in the Middle East and North Africa, while the affected area of droughts increased at high latitudes. Particularly, the Amazon, Nile and La Plata basins generally have experienced severer droughts than other basins. Meanwhile, the drought affected area and severity generally increase with duration over most basins.

1. Introduction

Drought is considered as the costliest disaster among natural catastrophes, which can lead to several negative effects on ecology, economy, and environment (Ha et al., 2022; Li et al., 2021; Lingfeng et al., 2022; Nguyen et al., 2021). For examples, the 2012 U.S. drought was a historically extreme event, causing over $30 billion in economic losses (Basara et al., 2019). In Yunnan, China, the most recent drought event occurred in 2018–2020, causing an economic loss of $240 million. Compared to other natural disasters, drought has higher lag time impacts (Angeline et al., 2020; Ha et al., 2022; Mishra & Singh, 2010). Under climate change, the intensity and unpredictability of drought is continuing to increase, with larger fluctuations than past (Yang et al., 2020). In this regard, the understanding of drought characteristics contributes to drought forecasting and management (Wu et al., 2022).

Drought indicators are effective tools for studying the evolutionary characteristics of drought. Various drought indices have been developed to carrying out drought monitoring and risk assessments. Meteorological drought is usually measured by the standardized precipitation index (SPI) (McKee et al., 1993, 1995). The SPI index has been widely used due to its simple calculation method and flexibility of time scale. However, it only utilizes precipitation information in the SPI calculation, and the role of temperature is ignored. In addition to SPI, the Palmer Drought Severity Index (PDSI) (Palmer et al., 1965) and the Standardized Precipitation Evapotranspiration Index (SPEI) (Vicente-Serrano et al., 2010), calculated from precipitation and temperature data sets are also employed to monitor meteorological and agricultural droughts. PDSI was created by Palmer et al. (1965) in 1965

based on the soil water balance principle and added evaporation dispersion. It effectively solves regional drought monitoring and forecasting; however, it suffers from calibration cycles, spatial comparability limitations, and subjectivity in the definition of drought classes (Guttman et al., 1992; Yan et al., 2009). The SPEI created by Vicente-Serrano et al. (2010) is an innovation from the SPI index, defined as the difference between cumulative precipitation and cumulative potential evapotranspiration, and was found to be temperature sensitive. Considering the disadvantages of SPI, SPEI provides an additional advancement in drought recording by accounting for the role of temperature on drought severity through potential evapotranspiration (PET).

A wide range of researches have involved spatial and temporal variability of drought from regional to global scale. Due to global warming, a significant nonlinear increase in the severity, intensity, area and duration of drought is predicted for the global land during the 21st century (Y. Ji et al., 2023). In China, severe droughts are gradually increasing, while rapidly increased in southwest China (Yang et al., 2013). Future projections indicate that extreme and severe drought events in Northwest Africa will likely become more frequent due to climate change and precipitation deficits (Balting et al., 2021; Driouech et al., 2020). A broader study of drought trends in the contiguous United States shows that the percentage of drought areas declined before the 1990s and has increased since the 2011s. Most of the previous studies have identified drought events from one-or two-dimensional perspective, which is inadequate to provide a comprehensive description of droughts as their spatial extents and geographical locations change over time. Indeed, drought is a three-dimensional phenomenon considering longitude, latitude and time, which requires a three-dimensional clustering algorithm to characterize (Andreadis et al., 2005). In addition, compared to regional studies, global studies enable direct comparison of drought characteristics in different regions, providing a broad picture of drought spatial and temporal distributions. Moreover, the understanding of meteorological drought from a basin perspective provides a direct guide for water resources management, as meteorological drought is usually the precondition of hydrological drought. Up to date, however, there is a lack of systematic study on meteorological droughts in global river basins, hampering a comparison of drought patterns between different river basins, and limiting governors or river managers from making drought adaptation and mitigation strategies appropriate for each basin.

In this study, we devoted to providing a comprehensive picture of spatial and temporal patterns of drought across 59 global major river basins during 1979–2020, by employing SPEI drought index and a three-dimensional clustering method, along with a discussion on the comparison between different drought indices. The rest of the paper is organized as follows. Section 2 describes the data sets and methods used, and Section 3 shows how well the three-dimensional clustering method is capable of capturing drought, after which drought spatial and temporal variations are analyzed. Section 4 compares the drought identification results of other indices and, finally, some conclusions are given in Section 5.

2. Methodology and Data

2.1. Drought Indices

A common variant of the SPI is the SPEI, which is very similar to the SPI and is widely used in drought studies. SPI determines meteorological drought based on precipitation, whereas the SPEI incorporates the Potential Evapotranspiration (PET) parameter, which makes the calculation more complex (Beguería et al., 2014). Previous studies have shown that the SPEI performs better compared to other indices for different regions particularly in arid regions (Almeida-Ñauñay et al., 2022; G. Ji et al., 2021; Soh et al., 2018; Zarei et al., 2021). Here we chose SPEI with a time scale of 3 months (SPEI-3) as it is representative of seasonal drought changes and is widely used in drought detection worldwide (Jiao et al., 2021; Khadka et al., 2021; Mishra & Singh, 2010). Commonly, a threshold of −1 was chosen to identify drought event (McKee et al., 1993; Rhee & Im, 2017), and classification of drought with different grades is shown in Table S1 in Supporting Information S1.

2.2. Drought Event Identification and Characterization

This study calculated drought indices for each grid using a three-dimensional clustering identification method (Andreadis et al., 2005). This method aims to identifying spatiotemporally continuous drought events with the help of three-dimensional array (latitude-longitude-time) of the drought index. Detailed steps are as follows:

Step 1: drought patches were delineated in each basin for each time step. According to the clustering algorithm of Xu et al. (2015) and Y. Ji et al. (2023), spatially adjacent drought grid points (SPEI less than −1) were

extracted and classified into independent drought patches. This process was repeated throughout the study period. Drought patches were retained only if their area was greater than a prescribed threshold. Following Sheffield et al. (2009), Lloyd-Hughes (2012), and Herrera-Estrada and Diffenbaugh (2019), a threshold of 500,000 km^2 has been used to analyze global drought over an area of 10 million km^2. Therefore, the area threshold was defined as 5% of the basin area was selected in this study.

Step 2: Categorization of temporally continuous drought events. If the overlapping area between two drought patches in adjacent months is greater than the threshold area, then the two patches are considered to belong to the same three-dimensional drought event cluster and are marked as the same drought event. Otherwise, they are marked as two separate drought events. This process is repeated until all drought patches are marked.

Step 3: Determine drought events throughout the study period. For the entire study period, step 2 was repeated until all drought events were identified. Finally, all drought events were identified as a series of contiguous drought patches.

In this study, five indicators were used to characterize drought events, including duration, area, severity, intensity, and drought centroid (Li et al., 2020). Drought duration is defined as the number of consecutive months during which a drought event lasts, and drought area is defined as the area affected by the drought event. Severity refers to the temporal accumulation of SPEI values of all drought grids in a 3D drought event, while intensity was defined as the average severity over a period of time and drought area for a drought event. Drought centroid is the weighted center in the three-dimensional drought cluster, which represents the latitude-longitude-time center of the drought event.

2.3. Data Source

The SPEI database covers the period between 1901 and 2020 with a spatial resolution of 0.5°. In this study, data were extracted for the 59 basins in a period of 42 years (1979–2020) at a monthly time scale. This data set is of good quality and widely used in drought studies (Jiao et al., 2021; Shi et al., 2022; Yu et al., 2023). For river basins, we focused on the major ones, namely the top 59 basins sorted by their drainage areas were selected. This is because according to relevant studies, it is possible that large-scale extreme drought occurs more frequently with global warming (Wu et al., 2023), thus selecting larger river basins for drought study can be more likely to capture large-scale extreme drought events. A schematic diagram of the 59 basins is shown in Figure S1 in Supporting Information S1.

3. Results

3.1. Climatology

The spatial patterns of drought severity, drought duration and drought intensity during 1979–2020 are presented in Figure 1, respectively. It is observed that there are three global drought centers, located in the Amazon basin of South America, northern Africa, and the central basin of Asia. Basin differences in the spatial distribution characteristics of SPEI are noticeable. The highest drought severity is observed in north-central Africa, the South American Amazon basin, and the Middle East. Northwestern Asia, south-central Europe, and central Oceania exhibited high drought severity, with an average severity ranging from 1 to 3 each month. The majority of basins experienced an average drought duration of 2–4 months, while the Congo basin, Amazon basin, and Tigris basin demonstrated prolonged durations. The spatial distribution of drought intensity closely mirrors that of drought duration. Analyzing the spatial distribution of mean drought duration in SPEI revealed that north-central Africa, the South American Amazon, the Middle East, and southwestern North America experience longer durations. The average duration in these basins exceeded 6 months. Drought severity, ranging from 1 to 4 in each month, was more intense in the northern part of North America, northern and south-central Africa, south-central Europe, and western Asia. From the spatial distribution of drought intensity, it can be seen that north-central Africa, the Amazon basin of South America, north-central Asia, are characterized by higher drought intensity.

Figure 2 presents the spatial distribution of drought centers in 59 river basins across continents. It illustrates that droughts characterized by long durations and high severity predominantly occur along the river courses in some specific basins, such as in Nile basin, Danube basin, and Ganges basin. In Asia, higher latitude basins such as Yenisey basin and Ob basin experience more frequent and severe long-lasting droughts compared to lower latitude areas. Drought events in Yellow river basin, St Lawrence basin, and Pearl basins are concentrated

10.1029/2024GL111442

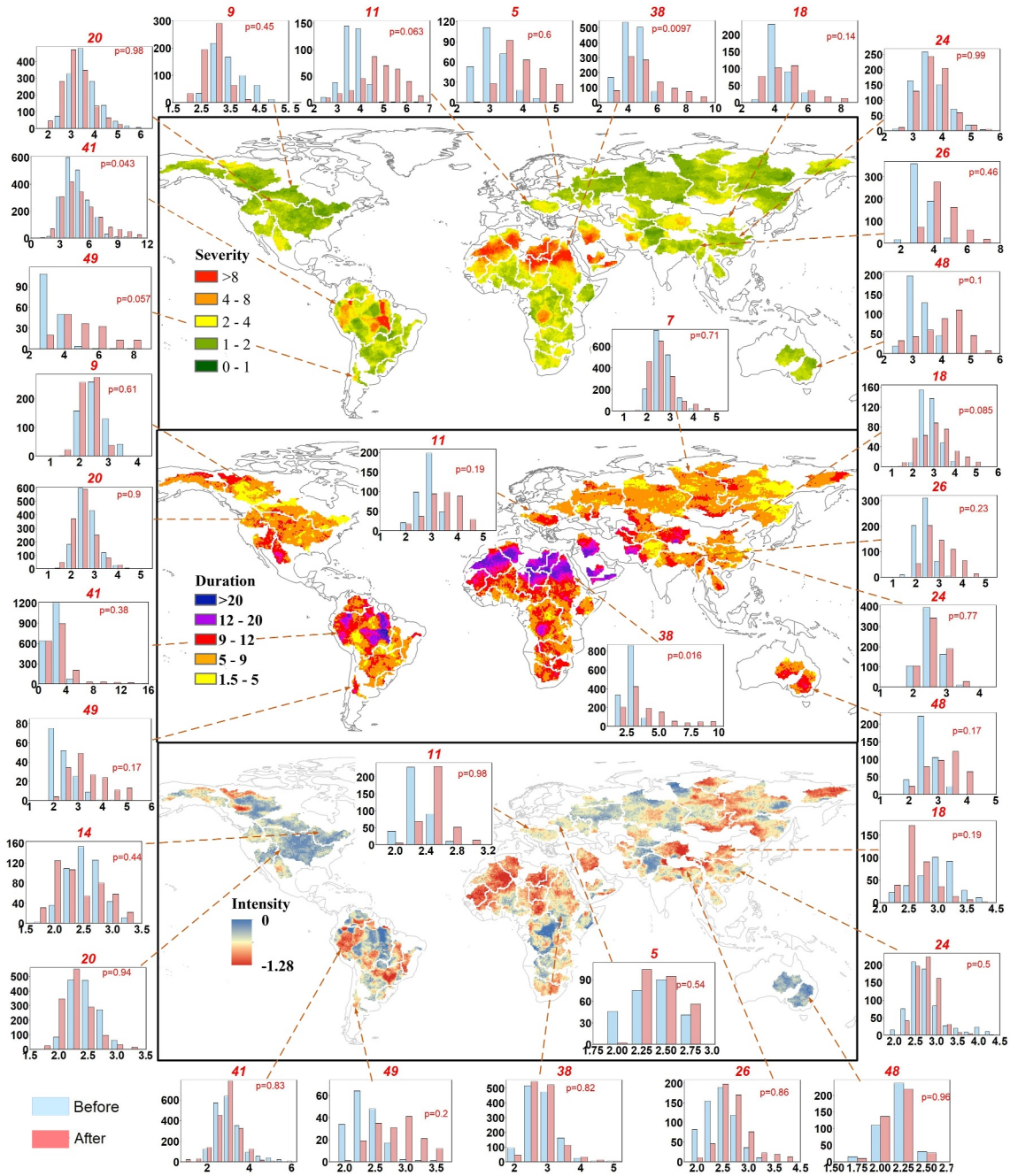

Figure 1. Climatology of drought severity, duration and intensity from 1979 to 2020 in the 59 river basins. Surrounding panels show the changes in distributions of drought severity, duration and intensity over 11 global typical basins in two sub periods, 1979–1999 and 2000–2020, in which p values from ANOVA test are given. The *x*-axis in each panel represents severity, duration and intensity of drought, respectively, and the *y*-axis represents number of drought events falling into a specific bin of frequency/severity/duration/intensity. The number on the top of each panel indicates basin code.

predominantly in the western parts of these basins, aligning with existing research (Fischer et al., 2011; Shi et al., 2022). Despite their small size, basins in the Middle East witness numerous long-lasting and severe droughts. In Ganges basin, the majority of drought events occurred in the central part of the basin. In Europe, larger basins notably experienced more long-lasting and severe drought events compared to smaller basins, with most drought events in Volga basin occurring in the central and western parts. In North America, it was evident that Mackenzie basin experiences significantly more long-lasting and severe drought events than other basins. In Africa, almost all basins in the northern Sahara witnessed numerous droughts in terms of duration and severity.

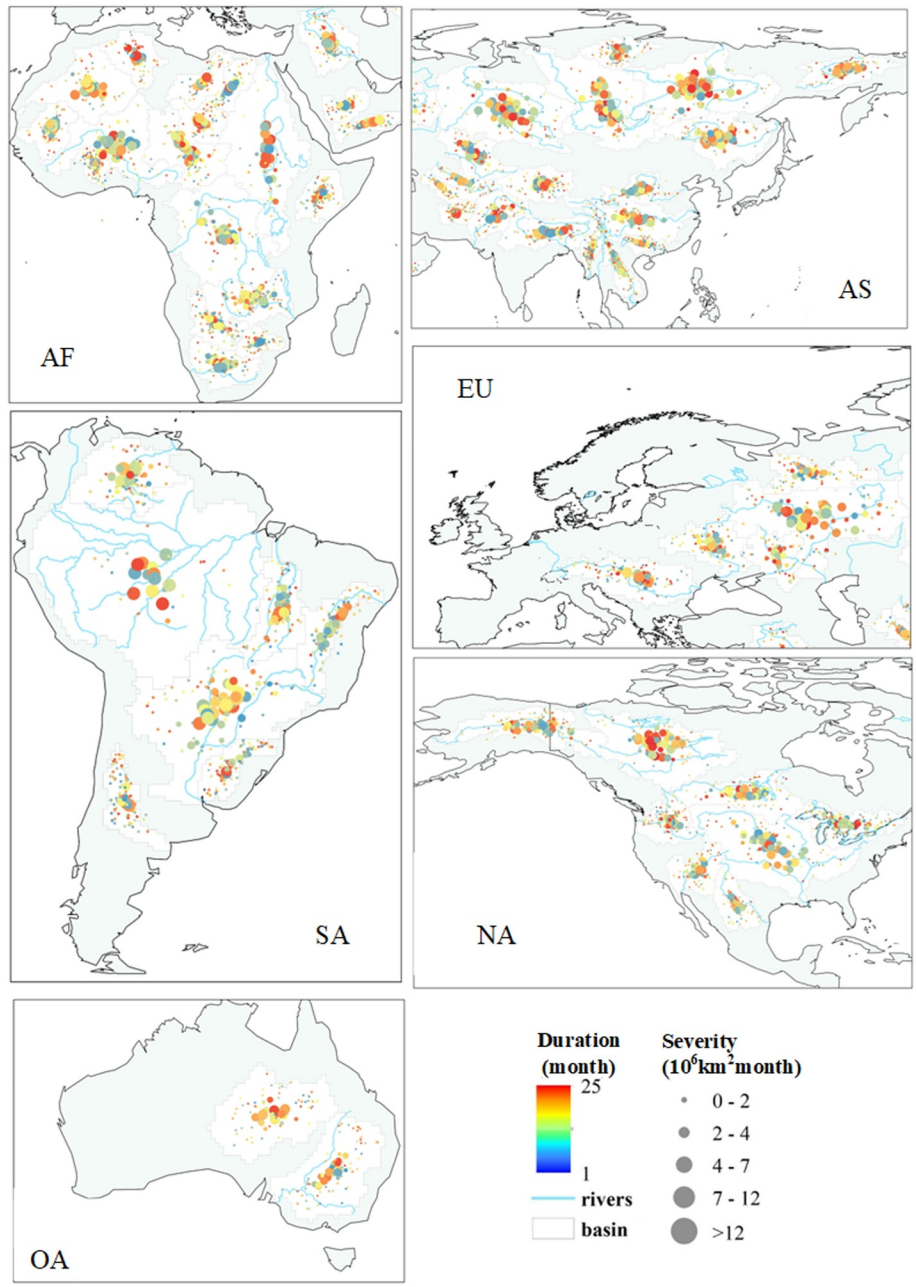

Figure 2. Spatial distributions of drought event characteristics across different basins during 1979-2020. Colors and sizes of the circles represent the duration and severity of drought events, respectively. The letter in each panel is the abbreviation of continent name.

Drought events in the Nile basin and Niger basin were severer in terms of severity than in other basins, while in southern Africa, short-duration but severe drought events were more common. In South America, it was noteworthy that drought events in both the Amazon basin and La Plata basin tended to be long-lasting and particularly severe. Drought events in the southern basins clearly followed the river courses. In Australia, drought events were generally shorter and less severe compared to other continents, mainly concentrated in the central parts of the basins. The inland river Great Artesian Basin experiences longer durations and higher intensities of drought compared to the Murray basin, a trend also observed in the inland rivers of the Middle East and Asia, which tended to have higher durations and severity compared to coastal basins. Overall, the central part of almost all basins was affected by drought events of long durations and large affected areas. The droughts in different basins

often occur on one side of the basin, such as the southwest side of the Yangtze basin and Yellow River basin. It is important to note that in the Nile basin, drought centroid exhibited a distinct distribution along the major river reach. Moreover, it is found that droughts in large and medium basins were generally more persistent and severe than in small basins (Table S3 in Supporting Information S1).

3.2. Temporal Changes

To investigate how drought evolved over time, we examined the changes in drought frequency, duration, severity and intensity between two sub periods, 1979–2000 and 2001–2020. The surrounding panels in Figure 1 and Figure S2 in Supporting Information S1 together presented histograms of drought frequency, severity, duration, and intensity distributions for the two periods over 11 typical/well known basins such as the Nile basin, Amazon basin and Mississippi basins (the remaining basins are in Figures S3–S6 in Supporting Information S1). In South America and Central Africa, most basins exhibited little change in drought characteristics between two periods, especially in the Amazon basin and Rio Grande basin. In Asia, drought frequency also displayed insignificant changes between two periods, particularly in the Yangtze basin, Yellow River basin, and Ganges basin. In Europe, some basins exhibited a stable drought frequency change, such as the Dnieper basin and Volga basin, while others, like the Don basin ($p < 0.1$), showed a tendency toward higher drought frequency. In North American basins, significant decreased drought frequency in the Yukon basin was found, whereas the Columbia basin showed oppositely ($p < 0.1$). It's worth noting that drought severity showed an increasing trend in Africa and South America, especially in the Congo basin ($p < 0.1$). The change in drought severity slightly differed from those in North America and South America. In the Middle East and north Africa, drought severity displayed a decreasing trend, particularly in the Shati ($p < 0.1$) and Ayeyarwady basin ($p < 0.1$), while other basins showed insignificant patterns. As for drought duration, many basins demonstrated a stable change, while the basins in Central Africa such as Chari basin ($p < 0.05$), Nile basin ($p < 0.05$) and Congo basin ($p < 0.1$) demonstrated increasing trends. Drought intensities between two sub periods were not significant in most basins, except for Congo Basin ($p < 0.1$) and Chari basin ($p < 0.1$) which showed a tendency toward decreasing trend. Overall, the change in drought characteristics between two sub periods was not significant in most cases.

3.3. Major Drought Events Space-Time Patterns

The aforementioned analyses were based on drought events with different grades. Yet, it was important to further look at major drought events as they pose much more threat to the society and ecosystem than moderate drought events. We thus selected events generally had large affecting area, high intensity and severity, and long duration. Additionally, based on the basin area and the population affected, all basins were categorized as large-, medium-, and small-sized, of which there were six large basins, 11 medium basins, and 42 small basins. More specifically, large basins were mainly classified as areas larger than 3 million km^2, while medium basins were classified as areas larger than 1 million km^2 but smaller than 3 million km^2, and the rest were classified as small basins. Table S2 in Supporting Information S1 listed the most severe drought events for 59 basins by basin code order and Figure 3 illustrated the spatiotemporal evolution of drought events in six large basins, which were divided into four stages. Clearly, the drought period of Danube basin began in October 1989 and ended in August 1990, lasting 11 months. The event started in the northwestern portion of the basin, whose center gradually moved southward and grew to a maximum in the north-central part of the basin, ultimately lingering and ending in the central mainstream. The drought event in the Mississippi basin (from December 2010 to November 2011) originated in the northern part of the basin, and then moved to southward, rapidly developing into a basin-wide drought and finally weakening in the north. The Yangtze basin experienced a 12-month drought from February 1997 to January 1998, originating in the western part of the basin, sweeping from the North China Plain to the middle reaches of the Yangtze River basin, and eventually weakening in the southwest basin, quickly reaching maximum intensity. As for the Amazon Basin, the drought event (January 2005–December 2005) originated in the eastern mainstem of the basin, weakening slightly as they moved westward, and then reached to the peak and eventually dissipated in the west. The Orange basin experienced a 11-month drought from April 1994 to March 1995, which originated in the western part of the basin, then progressed as it moved to the east, eventually peaking in the east and northwest and dissipating quickly. The drought event in Murray basin occurred from March 2019 through February 2020, with a cluster of three-dimensional droughts originating in the southern portion of the basin, weakening slightly in the eastern portion of the basin, and rapidly progressing to a basin-wide drought.

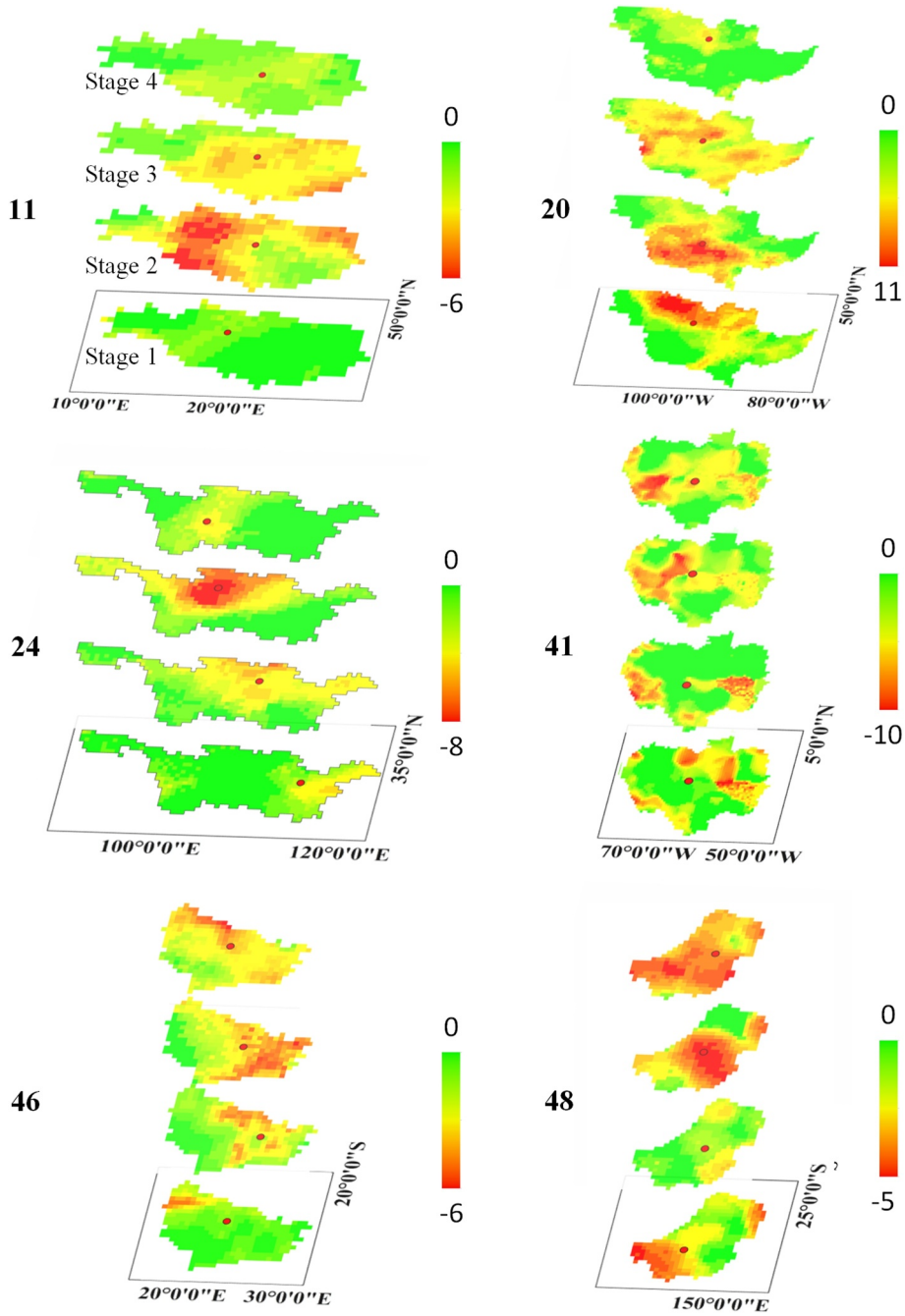

Figure 3. Spatiotemporal track of typical drought events in six large basins. The numbers at the left of each panel are basin codes. Red dots indicate the location of drought centers. Four drought developmental stages are initiation, development, peak stage, and vanish stage. The color bar shows the cumulate SPEI-3 during the drought event.

The spatiotemporal development of the major drought events in small and medium-sized basins had certain similar patterns (Figures S7 and S8 in Supporting Information S1). The major drought centroid movements revealed the development of most drought events, exhibiting a certain spatial cycle with the drought center swinging back and forth in local areas. Such pattern was typical in most basins, such as the Amazon basin, Yenisey basin and Shati basin, where major drought events returned to almost the same position after a year of movement. On the other hand, drought events in some basins exhibited clear and long pathway sweeping almost

the entire basin within a year, such as the Great Artesian Basin and Arabian Peninsula basin. It is interesting that in Ob basin, Colorado basin, and La Plata basin, drought centers moved over time in the direction of rivers.

4. Discussion

4.1. Relationship Between Drought Indicators

Figure S9 in Supporting Information S1 illustrated the relationship between the affected area (A), severity (S), intensity (I), and duration (D) of droughts for six large basins and the remaining basins are shown in the Figure S10 in Supporting Information S1. We employed power functions to fit the A-D and S-D curves for all basins, and the determination coefficients for all basin fits were above 0.85 indicating satisfactory fittings. Our findings revealed that the A-D curves for nearly all basins initially exhibited an increasing trend before stabilizing. The increase aligned more closely with a logarithmic relationship with duration, except for the Congo basin, which approximated a more linear growth trend. Meanwhile, S-D curves for most basins demonstrated a continuous upward trend, consistent with an exponential growth pattern. For certain basins, particularly the North African Sahara basin (such as Shati basin and Lake Chad basin), the Middle East (like Mekong basin), and central Australia (Great Artesian Basin), as well as some high-latitude basins (such as Yukon basin, Volga basin, and Northern Dvina basin), showed a sustained upward and linear trend. This pattern was attributed to these basins being situated in arid regions where the increase in drought severity with duration was weak. Notably, this trend was also observed in some monsoon-influenced basins, such as Yangtze basin, Ganges basin, and Danube basin. This discrepancy could be due to the significant influence of monsoons on rainfall in these basins. However, due to the limited occurrence of drought events lasting over 10 months, these curves entailed considerable uncertainty for long durations. Overall, the drought affected area and severity increased with the duration for most basins.

4.2. Comparison Between Different Drought Indices

It was necessary to compare the results between SPEI and other drought indices to explore the difference and similarities between indices in the identification of drought characteristics (Gumus, 2023; Meseguer-Ruiz et al., 2024). Therefore, we first adopted another widely used drought index, namely SPI, to perform the identification of meteorological droughts again, and the results are shown in Figures S11–S15 in Supporting Information S1, from which significant differences were observed between SPI-3 and SPEI-3 in terms of drought frequency. Notably, in South America and Central Africa, most basins exhibit significant strengthening trends, particularly in the Congo basin ($p < 0.1$), Tocantins basin ($p < 0.1$) and La Plata basin ($p < 0.1$). In Asia, many basins displayed a slight decrease trend, especially the Yangtze basin ($p < 0.1$). European basins mostly demonstrated unchanged drought frequency trend. In North America, all basins displayed same trends with those obtained from SPEI-3, except for the Colorado basin ($p < 0.1$) which exhibited a significant increase. The Middle East also displayed similar results with those of SPEI-3, while the Syr Darya basin experienced a decrease trend ($p < 0.1$). From Figure S16 and Table S4 in Supporting Information S1, it could be observed that the spatial distribution of drought events based on SPI-3 is basically the same as those based on SPEI-3, with the results of all drought events concentrating in the central part of the basins along river. In Asia, the spatial distribution of drought events detected by SPI-3 and SPEI-3 was the same. Droughts in different basins tended to occur near one side of the basin, such as in the Yangtze basin and Yellow River basin, where major drought events were generally concentrated on the southwest side. In Europe, there was little difference between the two indices, and it was noteworthy that drought events in Volga basin were mainly concentrated in the eastern part of the basin. In Africa, SPEI-3 detected more large-scale drought events in the middle and low latitudes. It was worth noting that drought events in the Nile River basin showed a clear distribution along the river, but this feature was not present in SPI-3. In North America, Mackenzie basin showed a significant difference, where SPEI-3 detected high severity and long duration of drought events, while SPI-3 showed results of shorter duration and lower severity. In South America, most notably in the Amazon basin, SPEI-3 monitors fared fewer drought events than SPI-3. As for the Oceania basin, there was no significant change in the two indices. In summary, it was evident that compared to SPI-3, SPEI-3 detected more large-scale drought events in low and mid latitudes, such as the Ganges basin and Mekong basin. This may indicate that droughts in low and mid latitudes were more sensitive to temperature. Figure S17 in Supporting Information S1 further illustrated the relationships among the affected area(A), severity (S), intensity(I), and duration(D) of drought events. The results showed that SPI-3 results were same to SPEI-3, and the drought area in most basins exhibited a linear increasing trend over time, followed by a tendency to

stability. The severity of drought varied in different basins, with most showing a linear increasing trend. In terms of drought intensity, most basins demonstrated a steady decrease.

We also compared SPEIs with different time scales, that is, SPEI-1, SPEI-3, SPEI-6, and SPIE-12, and a hydrological drought index, that is, standardized runoff index (SRI), to see how different the results are, and to enhance the understanding of drought characteristics from both meteorological and hydrological perspectives. Drought climatology, as presented in Figure S18 in Supporting Information S1, displays similar patterns among different SPEIs and SRI. Further, we selected five large basins across different continents to track drought events through these indices, and found that drought duration and magnitude somewhat differ among different drought indices, with drought duration increases while intensity declines as the SPEI time scale increases. While the spatial distribution of SRI shows similar pattern compared to SPEI-3, it has lower frequency and severity together with shorter duration in northern Africa and western North America (Figure S19 in Supporting Information S1). These findings indicate that the spatiotemporal patterns of drought climatology for different drought indices are similar, yet regionally there is certain difference in drought event characteristics.

5. Conclusions

In this paper, a 3D clustering algorithm was used to identify meteorological drought events based on SPEI from 1979 to 2020 over 59 global river basins. Five drought characteristic indicators including drought duration, affected area, severity, intensity and centroid were employed to analyze the spatiotemporal variations of droughts. It is found that the three-dimensional clustering method can capture the space-time structure of drought events. The severity, intensity and duration of droughts did not change significantly over time in most of the basins, while drought frequency showed a decreasing trend in the Middle East and North Africa basins and an increasing trend in high- and low-latitude basins. Notably, in the Amazon, Nile and La Plata basins, droughts generally tended to have higher severities. Moreover, severe droughts in most of large basins developed slowly over time but showed rapid disappearance during the fading stage. We also found that for most basins, drought affected area and severity both increased with duration.

Data Availability Statement

This study uses publicly available data only. 1–12 month time-scale of SPEIs were obtained from Consejo Superior de Investigaciones Cientificas (CSIC) (https://digital.csic.es/handle/10261/268088). The precipitation data used to calculate SPI3 was provided by the Climate Prediction Center (CPC) (Xie et al., 2007) and available from National Oceanic and Atmospheric Administration (NOAA) (https://psl.noaa.gov/data/gridded/data.cpc.globalprecip.html). The runoff data used to calculate the SRI were obtained from the Global RUNoff ENSEMBLE (G-RUN ENSEMBLE) (Ghiggi et al., 2021) and can be freely downloaded at https://figshare.com/articles/dataset/G-RUN_ENSEMBLE/12794075. Moreover, statistical analyses were conducted on the R platform (http://www.R-project.org).

Acknowledgments
This research was financially supported by the National Natural Science Foundation of China (52479015, 52109019), the Fundamental Research Funds for the Central Universities (2024ZYGXZR084), and the Natural Science Foundation of Guangdong Province (2023A1515030191).

References

Almeida-Ñauñay, A. F., Villeta, M., Quemada, M., & Tarquis, A. M. (2022). Assessment of drought indexes on different time scales: A case in Semiarid Mediterranean Grasslands. *Remote Sensing*, *14*(3), 565. https://doi.org/10.3390/rs14030565

Andreadis, K. M., Clark, E. A., Wood, A. W., Hamlet, A. F., & Lettenmaier, D. P. (2005). Twentieth-century drought in the conterminous United States. *Journal of Hydrometeorology*, *6*(6), 985–1001. https://doi.org/10.1175/jhm450.1

Angeline, G. P., Gerald, A. M., Roger, P., Hobbins, M., Hoell, A., AghaKouchak, A., et al. (2020). Flash droughts present a new challenge for subseasonal-to-seasonal prediction. *Nature Climate Change*, *10*(3), 191–199. https://doi.org/10.1038/s41558-020-0709-0

Balting, D. F., AghaKouchak, A., Lohmann, G., & Ionita, M. (2021). Northern Hemisphere drought risk in a warming climate. *npj Climate and Atmospheric Science*, *4*, 1–13. https://doi.org/10.1038/s41612-021-00218-2

Basara, J. B., Christian, J. I., Wakefield, R. A., Otkin, J. A., Hunt, E. H., & Brown, D. P. (2019). The evolution, propagation, and spread of flash drought in the Central United States during 2012. *Environmental Research Letters*, *14*(8), 084003. https://doi.org/10.1088/1748-9326/ab2cc0

Beguería, S., Vicente-Serrano, S. M., Reig, F., & Latorre, B. (2014). Standardized precipitation evapotranspiration index (SPEI) revisited: Parameter fitting, evapotranspiration models, tools, datasets and drought monitoring. *International Journal of Climatology*, *34*(10), 3001–3023. https://doi.org/10.1002/joc.3887

Driouech, F., ElRhaz, K., Moufouma-Okia, W., Arjdal, K., & Balhane, S. (2020). Assessing future changes of climate extreme events in the CORDEX-MENA region using regional climate model ALADIN-climate. *Earth System and Environment*, *4*(3), 477–492. https://doi.org/10.1007/s41748-020-00169-3

Fischer, T., Gemmer, M., Lüliu, L., & Buda, S. (2011). Temperature and precipitation trends and dryness/wetness pattern in the Zhujiang River Basin, South China, 1961–2007. *Quaternary International*, *244*(2), 138–148. https://doi.org/10.1016/j.quaint.2010.08.010

Ghiggi, G., Humphrey, V., Seneviratne, S. I., & Gudmundsson, L. (2021). G-RUN ENSEMBLE: A multi-forcing observation-based global runoff reanalysis. *Water Resources Research*, *57*(5). https://doi.org/10.1029/2020WR028787

Gumus, V. (2023). Evaluating the effect of the SPI and SPEI methods on drought monitoring over Turkey. *Journal of Hydrology*, *626*(Part B), 130386. https://doi.org/10.1016/j.jhydrol.2023.130386

Guttman, N. B., Wallis, J. R., & Hosking, J. R. M. (1992). Evaluating spatial comparability in the Palmer drought severity index. *Journal of the American Water Resources Association*, *28*(6), 1111–1119. https://doi.org/10.1111/j.1752-1688.1992.tb04022.x

Ha, T. V., Huth, J., Bachofer, F., & Kuenzer, C. (2022). A review of Earth observation-based drought studies in southeast Asia. *Remote Sensing*, *14*(12), 3763. https://doi.org/10.3390/rs14153763

Herrera-Estrada, J. E., & Diffenbaugh, N. S. (2019). Landfalling droughts: Global tracking of moisture deficits from the oceans onto land. *Water Resources Research*, *56*(9), e2019WR026877. https://doi.org/10.1029/2019wr026877

Ji, G., Lai, Z., Yan, D., Wu, L., & Wang, Z. (2021). Spatiotemporal patterns of future meteorological drought in the Yellow River Basin based on SPEI under RCP scenarios. *International Journal of Climate Change Strategies and Management*, *14*(12021), 1756–8692. https://doi.org/10.1108/ijccsm-01-2021-0004

Ji, Y., Fu, J., Lu, Y., & Liu, B. (2023). Three-dimensional-based global drought projection under global warming tendency. *Atmospheric Research*, *291*(106812), 0169–8095. https://doi.org/10.1016/j.atmosres.2023.106812

Jiao, W., Wang, L., Smith, W. K., Chang, Q., Wang, H., & D' Odorico, P. (2021). Observed increasing water constraint on vegetation growth over the last three decades. *Nature Communications*, *12*(1), 3777. https://doi.org/10.1038/s41467-021-24016-9

Khadka, D., Babel, M. S., Shrestha, S., Virdis, S. G., & Collins, M. (2021). Multivariate and multi-temporal analysis of meteorological drought in the northeast of Thailand. *Weather and Climate Extremes*, *34*, 100399. https://doi.org/10.1016/j.wace.2021.100399

Li, J., Wang, Z., Wu, X., Zscheischler, J., Guo, S., & Chen, X. (2021). A standardized index for assessing sub-monthly compound dry and hot conditions with application in China. *Hydrology and Earth System Sciences*, *25*(4), 1587–1601. https://doi.org/10.5194/hess-25-1587-2021

Li, L., She, D., Zheng, H., Lin, P., & Yang, Z.-L. (2020). Elucidating diverse drought characteristics from two meteorological drought indices (SPI and SPEI) in China. *Journal of Hydrometeorology*, *21*(6), 1513–1530. https://doi.org/10.1175/jhm-d-19-0290.1

Lingfeng, L., Bo, Q., Weidong, G., Yiping, Z., Qinghai, S., & Jiuyi, C. (2022). Phenological and physiological responses of the terrestrial ecosystem to the 2019 drought event in Southwest China: Insights from satellite measurements and the SSiB2 model. *International Journal of Applied Earth Observation and Geoinformation*, *111*, 102832. https://doi.org/10.1016/j.jag.2022.102832

Lloyd-Hughes, B. (2012). A spatio-temporal structure-based approach to drought characterisation. *International Journal of Climatology*, *31*(15), 2503–2519.

McKee, T. B., Doesken, N. J., & Kleist, J. (1993). Exploring the relationship between drought frequency, duration, and time scales. In *Proceedings of the 8th conference on applied climatology* (pp. 179–183).

McKee, T. B., Doesken, N. J., & Kleist, J. (1995). Monitoring drought across multiple time scales. In *9th conference on applied climatology/75th AMS annual meeting* (pp. 233–236). American Meteorological Society.

Meseguer-Ruiz, O., Serrano-Notivoli, R., Aránguiz-Acuña, A., Fuentealba, M., Nuñez-Hidalgo, I., Sarricolea, P., & Garreaud, R. (2024). Comparing SPI and SPEI to detect different precipitation and temperature regimes in Chile throughout the last four decades. *Atmospheric Research*, *297*, 107085. https://doi.org/10.1016/j.atmosres.2023.107085

Mishra, A. K., & Singh, V. P. (2010). A review of drought concepts. *Journal of Hydrology*, *391*(1–2), 202–216. https://doi.org/10.1016/j.jhydrol.2010.07.012

Nguyen, H., Wheeler, M. C., Hendon, H. H., Lim, E.-P., & Otkin, J. A. (2021). The 2019 flash droughts in subtropical eastern Australia and their association with large-scale climate drivers. *Weather, Climate, and Extreme Events*, *3*(2), 100144.

Palmer, W. C. (1965). *Meteorological drought. Research paper No. 45*. US Department of Commerce Weather Bureau.

Rhee, J., & Im, J. (2017). Meteorological drought forecasting for ungauged areas based on machine learning: Using long-range climate forecast and remote sensing data. *Agricultural and Forest Meteorology*, *237–238*, 105–122. https://doi.org/10.1016/j.agrformet.2017.02.01

Sheffield, J., Andreadis, K. M., Wood, E. F., & Lettenmaier, D. P. (2009). Global and continental drought in the second half of the twentieth century: Severity-area-duration analysis and temporal variability of large-scale events. *Journal of Climate*, *22*(8), 1962–1981. https://doi.org/10.1175/2008JCLI2722.1

Shi, H., Zhou, Z., Liu, L., & Liu, S. (2022). A global perspective on propagation from meteorological drought to hydrological drought during 1902–2014. *Atmospheric Research*, *280*, 106441. https://doi.org/10.1016/j.atmosres.2022.106441

Soh, Y. W., Koo, C., Huang, Y. F., & Fung, K. F. (2018). Application of artificial intelligence models for the prediction of standardized precipitation evapotranspiration index (SPEI) at Langat River Basin, Malaysia. *Computers and Electronics in Agriculture*, *44*(164–173), 0168–1699.

Vicente-Serrano, S. M., Beguería, S., & López-Moreno, J. I. (2010). A multiscalar drought index sensitive to global warming: The standardized precipitation evapotranspiration index. *Journal of Climate*, *23*(7), 1696–1718. https://doi.org/10.1175/2009jcli2909.1

Wu, X., Feng, X., Wang, Z., Chen, Y., & Deng, Z. (2023). Multi-source precipitation products assessment on drought monitoring across global major river basins. *Atmospheric Research*, *295*, 106982. https://doi.org/10.1016/j.atmosres.2023.106982

Wu, X., Guo, S., Qian, S., Wang, Z., Lai, C., Li, J., & Liu, P. (2022). Long-range precipitation forecast based on multipole and preceding fluctuations of sea surface temperature. *International Journal of Climatology*, *42*(15), 8024–8039. https://doi.org/10.1002/joc.7690

Xie, P., Yatagai, A., Chen, M., Hayasaka, T., Fukushima, Y., Liu, C., & Yang, S. (2007). A gauge-based analysis of daily precipitation over East Asia. *Journal of Hydrometeorology*, *8*(3), 607–626. https://doi.org/10.1175/JHM583.1

Xu, K., Yang, D., Yang, H., Li, Z., Qin, Y., & Shen, Y. (2015). Spatio-temporal variation of drought in China during 1961–2012: A climatic perspective. *Journal of Hydrology*, *526*, 253–264. https://doi.org/10.1016/j.jhydrol.2014.09.047

Yan, G. X., Lu, G. H., Wu, Z. Y., & Yang, Y. (2009). Integrating PDSI and SPI for a comprehensive meteorological drought index. *Water Resources and Hydropower Engineering*, *40*, 10–13.

Yang, P., Xiao, Z., Yang, J., & Liu, H. (2013). Characteristics of clustering extreme drought events in China during 1961–2010. *Acta Meteorologica Sinica*, *27*(2), 186–198. https://doi.org/10.1007/s13351-013-0204-x

Yang, P., Zhang, Y. Y., Xia, J., & Sun, S. X. (2020). Identification of drought events in the major basins of central asia based on a combined climatological deviation index from GRACE measurements. *Atmospheric Research*, *244*, 105015. https://doi.org/10.1016/j.atmosres.2020.105105

Yu, H., Wang, L., Zhang, J., & Chen, Y. (2023). A global drought-aridity index: The spatiotemporal standardized precipitation evapotranspiration index. *Ecological Indicators*, *153*, 110484. https://doi.org/10.1016/j.ecolind.2023.110484

Zarei, A. R., Shabani, A., & Moghimi, M. M. (2021). Accuracy assessment of the SPEI, RDI and SPI drought indices in regions of Iran with different climate conditions. *Pure and Applied Geophysics*, *178*(4), 1387–1403. https://doi.org/10.1007/s00024-021-02704-3